

# Stereochemistry and twisted crystals

Catherine E. Killalea and David B. Amabilino

School of Chemistry, The GSK Carbon Neutral Laboratories for Sustainable Chemistry, The University of Nottingham Triumph Road, Nottingham NG7 2TU, UK.

E-mail. david.amabilino@nottingham.ac.uk

## **Abstract**

This review article discusses a link between stereochemistry and structural and morphological chirality. We present the remarkably frequent, but less often reported, growth of twisted crystals and discuss the reasons for their formation and ways to favor their growth. The more commonly encountered conglomerates and racemic compounds can be formed by achiral molecules, but the emergence of morphological chirality is often not considered in this context and perhaps deserves attention. Twisted crystals are known for a wide variety of materials, molecular and macromolecular, complexes and oxides, and so on. In growing crystals, twisting of lamellae because of strain generated during growth eventually unwinds in larger objects, and may not be detected. This kind of chiral morphology arising from low symmetry growth, and the challenges and opportunities for research in the area, are highlighted. In particular, the link between structural bending in supramolecular aggregates in solution or at interfaces, chiral nanofilaments in liquid crystals, and chiral polymers, is discussed.

## Introduction

The famous enantiomorphic crystals formed by sodium ammonium tartrate<sup>[1,2]</sup> are visibly chiral. This fact, coupled with tremendous patience in the triage of the mirror image chiral crystals, allowed Louis Pasteur to reveal the existence of molecular chirality, and led to the discovery of biological enantioselectivity.<sup>[3]</sup> Since then, crystallography has continued to play a hugely important role in research into chiral systems.<sup>[4,5]</sup> Significant challenges and questions remain today, however, in understanding the reasons for the shapes of crystals.<sup>[6]</sup> In the case of enantiomorphs, like the enantiomers of sodium ammonium tartrate, the emergence of chiral morphologies was difficult to trace, largely (we suspect) because of the difficulties in unequivocally detecting mirror image crystal shapes. While we will see examples of inorganic materials whose chiral growth has been probed using electron microscopy, the situation for organic materials often remains very challenging. For mixtures of enantiomers of molecular compounds, triage of enantiomorphic crystals has been used for their separation<sup>[7,8]</sup> but easier ways of making chiral materials exist. The separation of enantiomers by other means (such as chromatography) leads to chiral building blocks that can be used to induce homochirality in crystallization,<sup>[9]</sup> for example in the remarkable Viedma ripening.<sup>[10,11]</sup> These methods can be far more efficient at separating enantiomers than triage. It also seems that (anecdotally at least) very few chiral compounds have enantiomorphic crystals, in which case triage based on crystal shape impossible.

Enantiomeric chiral compounds can induce the formation of chiral crystal morphology, and the emergence of asymmetry in crystals of achiral molecules has been linked to chirality in biological systems.<sup>[12]</sup> A beautiful example of the induction of chirality into crystal morphology is the use of polar or centrosymmetric materials to indicate the absolute configuration of chiral molecules in growth or dissolution media.<sup>[13]</sup> For example, when crystals of  $\{R,S\}$ -serine are grown, addition of (*R*)- or (*S*)-threonine affords enantiomorphic crystals because of the stereospecific inhibition of the development of certain faces caused by the additional methyl group in the chiral additive.<sup>[14]</sup> This kind of "tailor made" impurity modifies growth and allows the direct absolute configuration determination of chiral polar crystals<sup>[15]</sup> and the resolution of conglomerates.<sup>[16]</sup> It is a poignant demonstration of the control of crystal growth leading to new phenomena with potential applications.

Molecular chirality is not essential for the formation of enantiomorphic crystals, not even that forced by spontaneous resolution of achiral components to give chiral structures: Chiral morphologies emerge in the growth of otherwise achiral chemistry. This formation of twisted crystals was recognized in the 19<sup>th</sup> century (Figure 1).<sup>[17]</sup> Many examples were discovered and highlighted along with more contemporary discoveries in a review on

twisted and bending merging in crystal growth.<sup>[18]</sup> Indeed, twisting in crystal growth is proving to be a frequent phenomenon under certain conditions.<sup>[19]</sup> We aim to show here that while a twisted crystal might be considered an inconvenience for the scientist wishing to obtain a single crystal structure, the emergence of these exotic and beautiful morphologies raises fascinating challenges. These opportunities lie in crystal growth in general, and in the field of stereochemistry, in particular. This review, is motivated by unpublished results from our research and in honor of Leslie Leiserowitz and Meir Lahav for their amazing contributions to chiral crystallization.

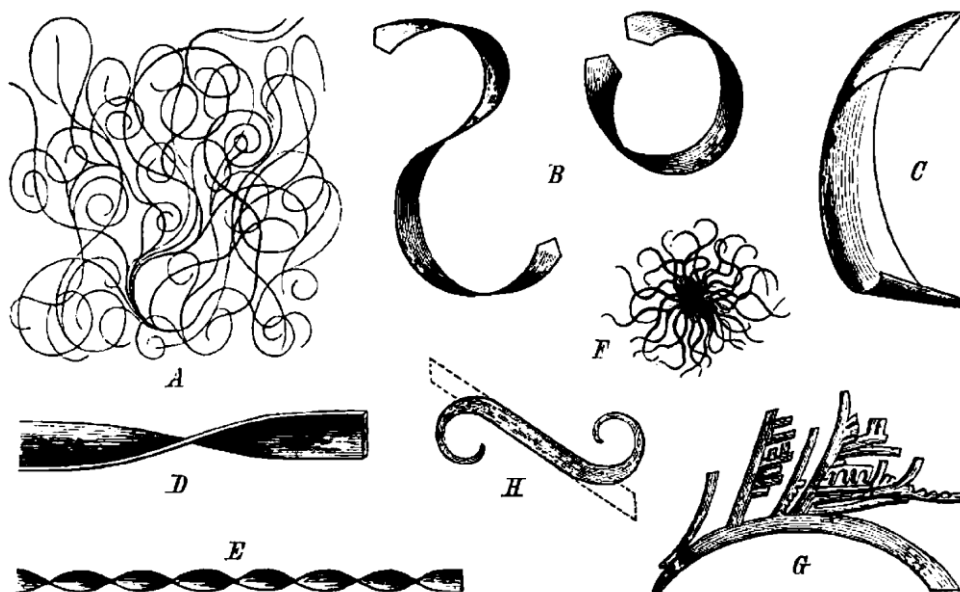


**Figure 1.** A selection of curves, curls, whorls, twists, scrolls and branches seen in crystals of a solid solution of the divalent chlorides of chromium and mercury (A), 1,2-diphenylethane-1,2-diyl diacetate (B), *Z*-cinnamic acid (C) potassium dichromate (D), hydroxyquinoline (E), the complex of aniline and 4-methyl-2,6-dinitrophenol (F) and 2,5-dihydroxy-3,6-dipropionylcyclohexa-2,5-diene-1,4-dione (G) by Lehmann in the 19<sup>th</sup> century [ref 17].

### Enantiomorphism and types of twist

Types of enantiomorphism include that evident in the crystal faces of three-dimensional objects (with similar sizes in all dimensions) and acicular solids. Large mineral crystals show a variety of chiral morphologies<sup>[20]</sup> that are presumably dependent on the very specific growth conditions at play when they were formed. Mesoscale twisted crystals of many substances were documented in the early 20<sup>th</sup> century.<sup>[19]</sup> This review concentrates on more recently discovered smaller objects where the crystals have one growth direction that is preferred to the others, giving enantiomorphic twisted solids.

Thin, flat crystals that have a high aspect ratio can in principle bend by distorting along two perpendicular directions in the plane of the ribbon-like object to afford tubes. Bending along the shorter axis generates a long narrow tube, and about the long axis generates a wide stubby cylinder. Bending along angles that do not coincide with the axes generates twisted objects (Figure 2). When the angle is closer to the longest axis of the object (lengthways bending), cylindrical helices are obtained while along the shorter axis twisted ribbons result (widthways bending). These objects correspond to a positive and negative curvature of the ribbon, respectively, and each kind of twisted object can be characterized by a pitch that depends on the degree of bending. Curving at opposite angles with respect to the principal axis will generate enantiomorphous objects. This intuitive analogy with a physical ribbon corresponds very well with objects seen in different kinds of crystallization.



**Figure 2.** Outcomes of twisting a flat ribbon sideways (upper objects) and lengthways (lower objects).

Apart from mesoscale crystals, highly ordered microscopic fibers exhibit these morphologies. Birefringent surfactant fibers were seen twisting using an optical

microscope over 75 years ago.<sup>[21]</sup> While lithium 12-hydroxystearate was noted to twist shortly afterwards,<sup>[22]</sup> it was much later that the sense of twisting was related directly with the chirality of the objects.<sup>[23]</sup> More recently, the induction of chirality in bilayer-forming dicationic gemini amphiphiles has been shown using tartrate anions.<sup>[24]</sup> The enantiomer and proportion of chiral anion determine the twist sense and pitch of the twisted ribbons that evolve over time. All these systems are formed in solution.

From melts of molecular materials, apparently chiral crystals grow with remarkable frequency, about 25% of simple molecular crystals.<sup>[19]</sup> That initial analysis was based on the observation of banded spherulites, which show concentric rings with alternating extinction effects when viewed between crossed polarizers in an optical microscope (the color change a result of the orientation of the lamellae and their extinction). The studies indicated that crystals emanated from a nucleation point radially while twisting helically around their main growth axis. Today's analytical methods have shown that the situation is more complicated, because rhythmic precipitation of undistorted crystallites can occur, in addition to spherulites of helical fibrils, and even a combination of both effects.<sup>[24]</sup> Nonetheless, a wide variety of inorganic,<sup>[25,26]</sup> polymeric<sup>[27,28]</sup> and simple organic molecular<sup>[29,30]</sup> materials form crystals with a twisted shape. Characterization of the morphological and structural details of the banded spherulites is facilitated, as before, with polarized optical microscopy, as well as transmission electron microscopy, X-ray diffraction and scanning probe microscopy. These techniques give hints to answer the key questions in these systems, how and why does twisting occur?

### **Explaining twisting during crystal growth**

The morphologies of twisted crystals observed in a wide variety of materials can be fitted to ribbon analogies, or be less simple. Thus, the origins of bending are not necessarily the same in every case, so in this section we present some of the hypotheses that have been forwarded to explain these situations.

The imperfect growth of straight single crystals can be attributed to the presence of dislocations in the crystal lattice,<sup>[31,32]</sup> where there is a linear change of the crystalline order on either side of the defect and the regular occurrence of these faults is readily extended to the theory of twisted crystal growth. In 1953, J. D. Eshelby<sup>[33]</sup> ascribed the growth of thin whiskers of tin to a screw dislocation parallel to the axis of the whiskers, an axial screw dislocation. In subsequent years, this "Eshelby twist" was applied to numerous relatively large inorganic fibrous crystals, including, sapphire (the alpha form of alumina),<sup>[34,35]</sup> lithium fluoride<sup>[36]</sup> and even sodium chloride.<sup>[37]</sup> More recently, Eshelby's mechanism has been demonstrated on the nanoscale in the growth of zinc oxide<sup>[38]</sup>, lead (II) selenide<sup>[39]</sup> and lead (II) sulfide nanowires.<sup>[40]</sup> The latter example shows elegantly the

features that can arise from this phenomenon. Structural characterization of the tree-like PbS nanowires grown by chemical vapor deposition and under vapor-liquid-solid conditions (Figure 3) revealed an axial screw dislocation in the trunks of the 'trees', which provided a driving force for the helically rotating epitaxial growth of nanowire branches.<sup>[41]</sup>

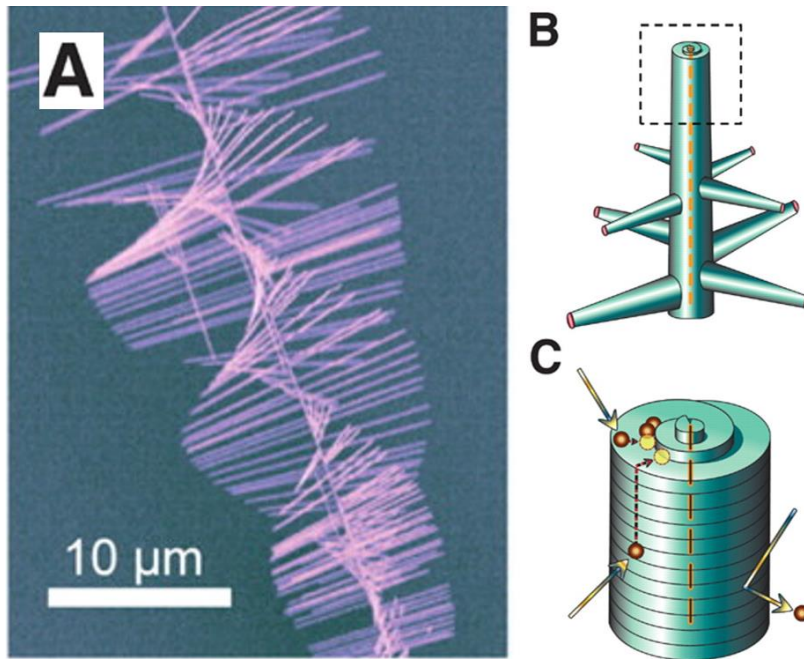


**Figure 3.** A) Tree-like PbS nanowires grown by the Eshelby mechanism. B) Cartoon illustration of the end of a PbS "tree", showing the axial placement of the lateral branches indicating the slow vapor-liquid-solid growth of the "branches" compared with relatively much quicker dislocation-driven growth of the core nanowire "trunk". C) A cartoon showing a spiral of an axial screw dislocation that self-perpetuate at the tip of the "trunks" of PbS nanowires. Reproduced and adapted with permission from ref 40.

Transverse screw dislocations have also been observed in twisted crystals, predominantly in polymer lamellae in spherulites, resulting in discontinuous twisting (Figure 4).<sup>[42-44]</sup> They are often observed at branching points,<sup>[44,45]</sup> although it has been argued<sup>[18]</sup> that these dislocations are a consequence of twisting and are a form of elastic stress relief rather than a cause of twisting because polymer lamellae with similar twisting pitch have been observed without these dislocations.<sup>[46]</sup>

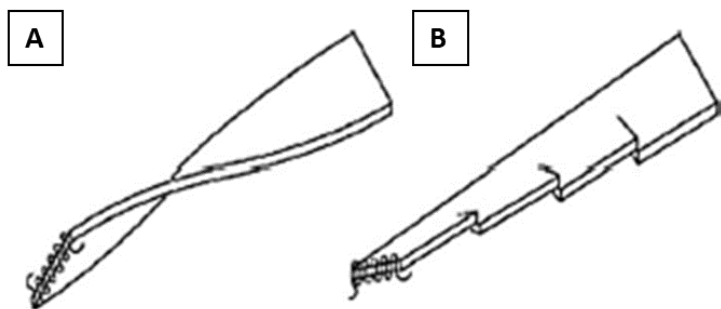


**Figure 4.** The results of transverse screw dislocations in polymers (the chains represented in the planes of the ribbons) leading to A) smooth continuous structures and (B) resulting from sequential homochiral axial screw dislocations. Reproduced with permission from ref. 45.

So, if transverse screw dislocations are a form of elastic stress relief, then where does the elastic stress originate? There are many inorganic materials that have polar non-centrosymmetric crystal structures and can grow into twisted nanoribbons that have broad polar faces. These polar faces develop surface charging, and the electrostatic energy is relieved at the expense of elastic energy by twisting or bending. A wide variety of helices,<sup>[47-49]</sup> rings<sup>[50,51]</sup> and even “nanowebbs”<sup>[52]</sup> have been grown in this way. The most widely studied material across the literature that forms twisted and coiled structures in this way is zinc oxide. ZnO has been shown under vapor-solid growth conditions to form spontaneous polarization-induced nano -helices<sup>[53-56]</sup> and -rings.<sup>[57]</sup> The nanohelices growth is dominated by oppositely charged  $\pm(0001)$  surfaces (terminated with  $\text{Zn}^{2+}$  and  $\text{O}^{2-}$ , respectively), resulting in a spontaneous polarization across the nanobelt thickness; the total energy of the system is minimized by coiling into helices that can reach lengths of 100  $\mu\text{m}$  (Figure 5).

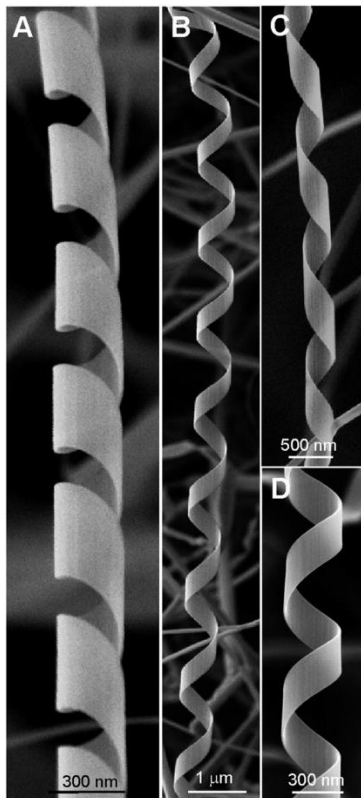


**Figure 5.** SEM micrographs of ZnO nanohelices, where (A) and (C) are left/handed, while (B) and (D) are right/handed. Reproduced with permission from ref. 55, Copyright 2005, American Association for the Advancement of Science.

For crystals that are not inherently polar, stresses at the crystal surface can still occur. For very thin objects, surface stresses can become exceedingly important in determining their morphology. Surface stresses predominantly occur in polymer lamellae, when polymer chains on the crystal interior differ from the arrangement of polymer chains at the surface, this can cause surface stress, when these surface stresses are unbalanced, the polymer lamellae twist to relieve the surface stress at the expense of elastic strain.<sup>[58,59]</sup> Polymer lamellar twisting can be easily observed through the periodic banding of spherulites when viewed through a polarized optical microscope (Figure 6) – polyethylene is one of the most extensively studied polymer spherulites.<sup>[60-64]</sup> In polyethylene, it is believed that when band spacing is small (<10 $\mu$ m) tilting of polymer chains within a lamella results in congested packing, more so on one side of the lamellae than the other, giving rise to twisting moments to relieve surface stresses. The surface stresses that occur as a result of the limited space can cause isochiral transverse screw dislocations which give rise to branching within the spherulite. This limits the available space further, augmenting the twisting that is observed.

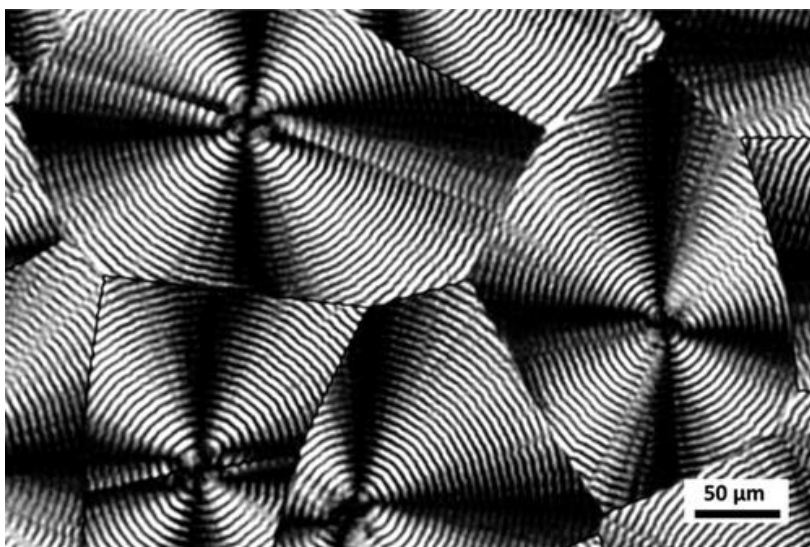


**Figure 6:** A polarized optical micrograph of crystalline polyethylene banded spherulites. Reproduced with permission from the American Chemical Society, ref [63].

More recent studies have established that spherulites grown from small molecules can also succumb to surface stresses, in the case of mannitol, lamellae in spherulites become twisted when grown in the presence of poly(vinylpyrrolidone) or sorbitol additives.<sup>[65]</sup> The banded spherulites grown shared essential qualities with polymeric spherulites in terms of size, shape and arrangement of lamellae, suggesting that their growth mechanism is similar to that of polymeric spherulites.

The growth of larger twisted crystals is commonly explained by the autodeformation mechanism. First proposed by Punin<sup>[66]</sup> to explain the existence of various crystal growth defects such as branching and twinning, it can also be applied to the growth of twisted crystals.<sup>[18]</sup> Autodeformation occurs when subvolumes (part of the evolving sample) of crystals growing at different times experience slightly different growth conditions. These differences in conditions can be a result of environmental gradients from inhomogeneous heat distributions, crystallization pressures or distribution of impurities. The result of any of these effects can lead to minor compositional differences in the subvolumes of a growing crystal. At the interface, where these subvolumes meet, there will be a difference in local lattice constants producing elastic strain and stress (heterometry stresses), which can be relieved by twisting or bending. Autodeformation as a result of heterometry stresses has been applied to multiple macroscopic twisted crystals including quartz<sup>[66]</sup> and gypsum.<sup>[67]</sup> The twisting of smaller more fibrous crystals have also been explained using the autodeformation mechanism – benzamide, the first organic molecule for which two polymorphs were discovered, has a metastable state in which it grows into strongly twisted aggregates.<sup>[68]</sup> (Figure 7).

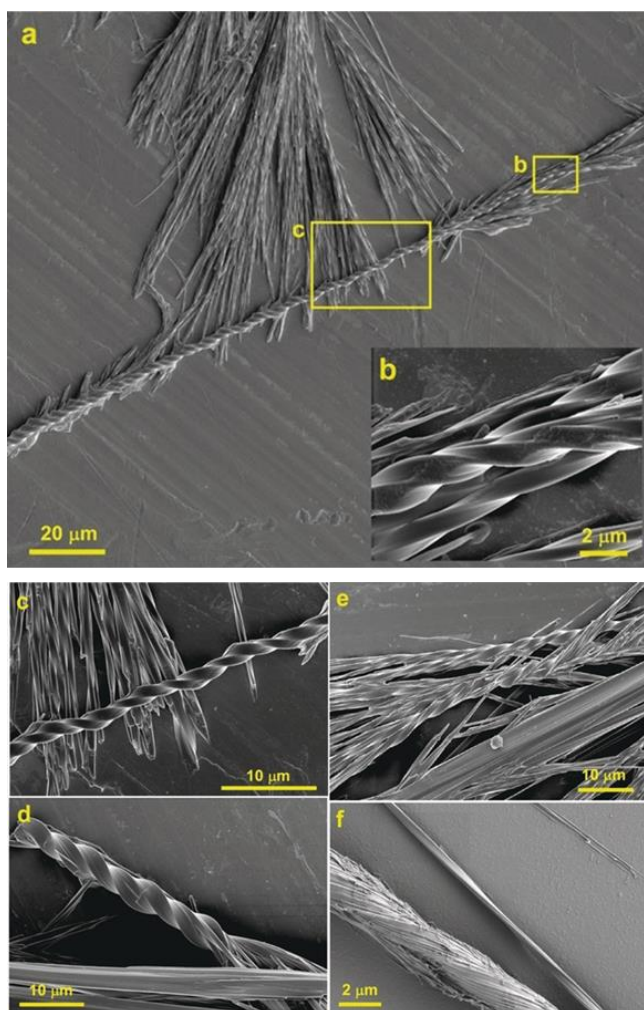


**Figure 7:** Scanning electron micrographs of strongly twisted crystals of benzamide II. Image a shows a very long and relatively thick twisted object with enlargement areas shown in b and c. The unbundling of strongly twisted crystallites is shown in d and e, where the formation of flatter and thinner needles is observed. The formation of thin needles by unbundling of a strongly twisted rope is shown in f. Images a-c were obtained from samples of benzamide grown from solutions containing L-arginine and d and e contained L-asparagine. Image f came from an experiment with no additives. Figure reproduced with permission from ref. 68.

The metastable benzamide crystals were grown in microdroplets in aqueous solution (20–30 mg mL<sup>-1</sup>) that were cooled relatively fast ( $\approx 1 \text{ }^\circ\text{C s}^{-1}$ ), giving a precipitate comprising twisted needles and some plates of the more stable polymorph. Microscopy studies revealed that the twisted benzamide crystals consist of many slightly misoriented crystallites and it was proposed that the orientation misalliance of these crystallites causes heterometry stresses generating a twist moment that is sufficient to generate the twisted morphology of this lamellar system.

A great range of substances can form twisted crystals with varying sizes, shapes and physical properties; the same substance can even form differing morphologies of twisted crystal when grown under different conditions.<sup>[65,69]</sup> No one mechanism fits all cases

unequivocally. In situations where a variety of explanations are plausible, it is likely that each can be suitably applied for a variety of materials that form under their own specific set of conditions. With incisive experiments, the choice of possible mechanisms for twisting may be narrowed down.

There are generally well-defined relationships between the twisting observed in the crystalline objects and their dimensions,<sup>[30]</sup> because the objects apparently unwind as they grow. For systems with apparent homochiral transversal dislocations a power function of the twist period  $P = kh^n$  can be fitted (Figure 8) where  $h$  is the smallest cross-sectional size and the value  $0.6 \leq n \leq 1.3$  are specific for the material and method of growth. The graph shows specific regions where particular materials have this relationship between pitch and smallest dimension,<sup>[28, 30, 70-75]</sup> the thickness of a ribbon for example. Where Eshelby twist arises (axial screw dislocations) the function  $P \sim h^2$ .<sup>[40]</sup>

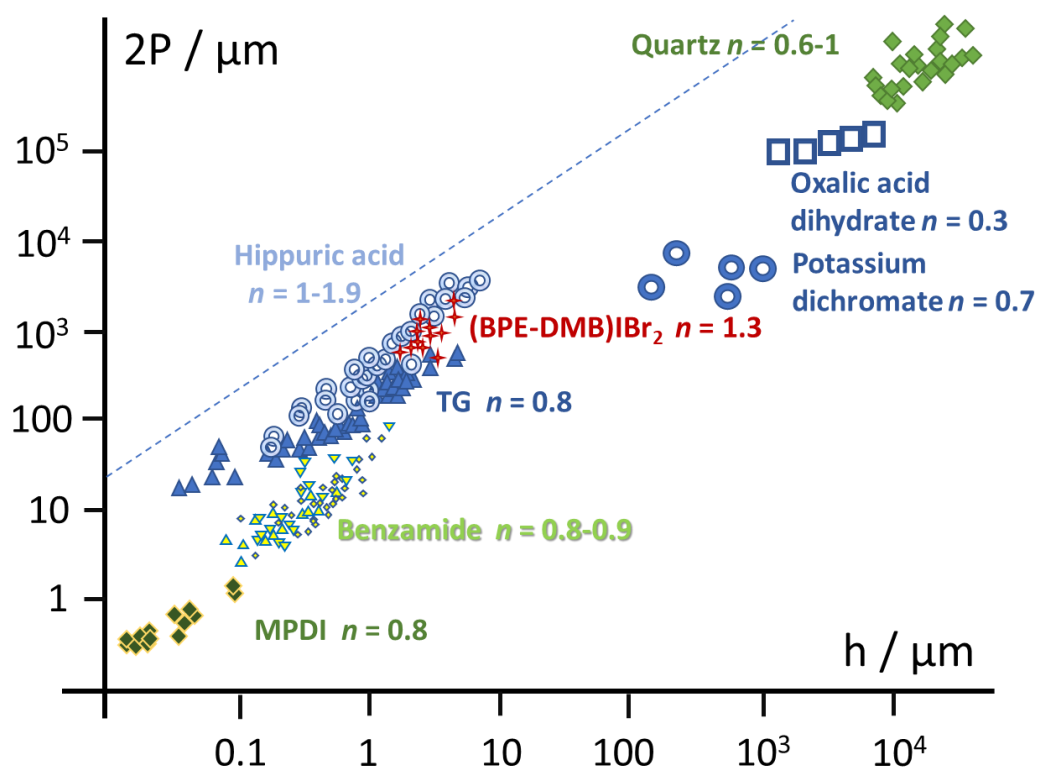


**Figure 8.** Correlation between full twist period ( $2P$ ,  $2n$  rotation,  $\mu\text{m}$ ) and the smallest crystal size in a cross section (for example, the thickness of a ribbon,  $h$ ,  $\mu\text{m}$ ). Data taken from the cited works for: Quartz;<sup>[70]</sup> oxalic acid dihydrate;<sup>[71]</sup> potassium dichromate;<sup>[72,73]</sup> (1,4-bis[2-(pyrene-1-yl) vinyl]-2,5-dimethylbenzene)IBr<sub>2</sub>, (BPE-DMB)IBr<sub>2</sub>;<sup>[74]</sup> hippuric acid (vapor grown);<sup>[75]</sup> *N*-(2-thienylcarbonyl)glycine, TG;<sup>[30]</sup> poly(*meta*-phenylene isophthalamide), MPDI.<sup>[28]</sup> For each material and condition, the exponent  $n$  can be determined from a fit to  $P = kh^n$ . The dashed line corresponds to  $2P < 10^3nh$ , below which (at least) partial relaxation of stress can relax in the twisted crystals.

### **Twisted aggregates, crystals and stereochemistry**

The reader whose main interest is in chiral compounds may have been surprised by the dominance of achiral systems in the discussion thus far. Many chiral supramolecular materials show chiral morphology, but the link with higher level twisting in irrefutably crystalline materials is less clear. Chiral and achiral compounds are frequently observed as chiral fibers with nanoscale dimensions, systems that have been reviewed thoroughly<sup>[76-78]</sup> although not in the context of chiral crystals. It has been pointed out before that there is a distinction between helical supramolecular aggregates and twisted crystals.<sup>[18]</sup> Definition of this frontier would be highly subjective. Twisted supramolecular nanoscale objects, very often formed by chiral amphiphiles that generate lamellar structures with solid or liquid character,<sup>[79]</sup> are not generally seen to grow into larger crystals with long range order, with or without twisting. These kinds of supramolecular assemblies are generally formed closer to equilibrium conditions than larger crystals, although nucleation and growth mechanisms can be similar.<sup>[80-82]</sup>

A particularly interesting case of twisted fibers are those formed from a synthetic amphiphilic peptide (Figure 9) that evolves from one kind of morphology to another over time.<sup>[83]</sup> When dissolved in ultrapure water at 25 °C twisted ribbons form quickly. Over the course of a month, they transform into cylindrical helices. The twisted ribbons (observed after about ten minutes) have a thickness between 5 and 6 nm and a width of around 20–40 nm; the helical pitch is 150–200 nm. The fibers have a high degree of order, giving X-ray diffraction peaks corresponding to spacings of 4.8 and 12.6 Å, akin to fibrillar protein aggregate order. Changing the nature and number of amino acids in the amphiphile changes the morphology displayed by the aggregates.<sup>[84]</sup> In general, this kind of bending in amphiphiles is believed to be driven (partially at least) by electrostatic interactions near the edge of the ribbons,<sup>[85]</sup> reminiscently of the inorganic helices that we highlighted earlier in this review.

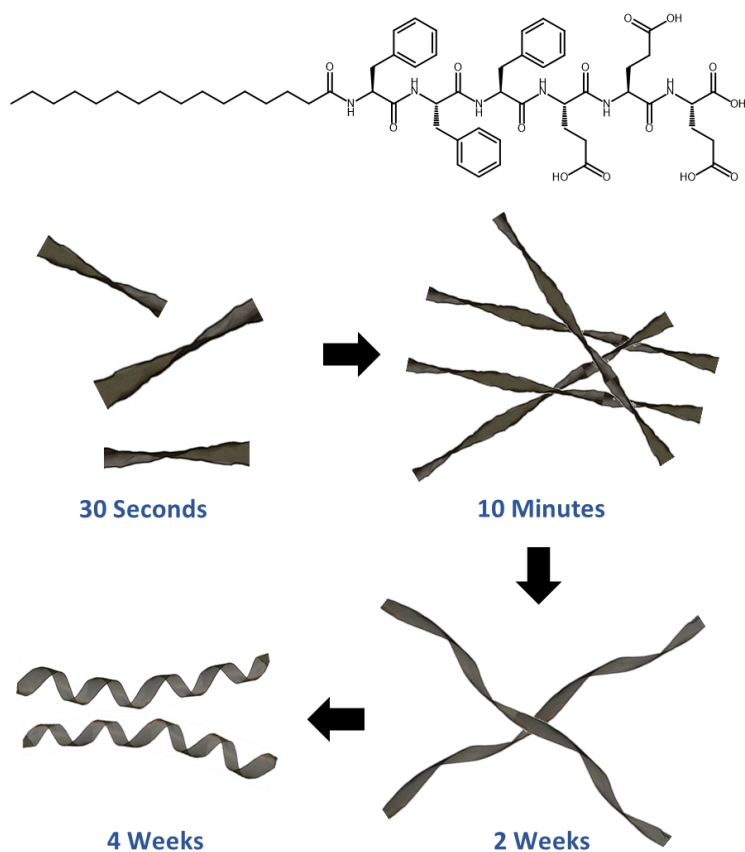


**Figure 9.** A synthetic peptide amphiphile that shows time/dependent twisted fiber morphology.<sup>[83]</sup>

The dimensions of twisted crystals seen for polymers are in the same size range as some self-assembled aggregates. Neither of these (generally lamellar type) objects grow into larger crystals. There seems to be no fundamental reason why lamellar structures, in general, should not follow similar mechanisms of twisting. Perhaps a future analysis of these systems will uncover a close connection between the two kinds of material. Indeed, bent-core mesogens are materials that can display phases that are essentially twisted crystals, most recently referred to as helical nanofilament phases.<sup>[86]</sup> Bending of smectic lamellae are the structural feature that allow the twisted filaments (that are around 25 nm wide and with half-pitch  $h \approx 100$  nm) to form. This particular example was based on an achiral material that undergoes spontaneous resolution of its conformational enantiomers in the mesophase, in common with similar materials.<sup>[87,88]</sup>

The constitution of the bent core family of compounds can be modified using chiral side chains that interact between lamellae. In a remarkable family of compounds, flat nanoribbons, twisted nano- and micro-filaments, and nanocylinder conglomerates form depending on the substitution pattern (Figure 10).<sup>[89]</sup> The compound lacking stereogenic centers forms a conglomerate of nanofibers as before, and introduction of chiral side chains

leads to stereoselective assembly. The lower symmetry compounds, with a chiral "tail" on one side of the molecule and achiral on the other, lead to microfilaments or nanocylinders as a consequence in the change of the interlayer interactions arising from the position of the stereogenic centers. The filament structures were ascertained using scanning and transmission electron microscopy, aided by synchrotron-based X-ray diffraction. Overall, it is the side of the molecule that is longer that determines the chirality of the filaments.<sup>[90]</sup> It is the relative discrepancy between the sides that are 3- or 4-substituted at the central dioxybiphenyl core that determine the morphological outcome.

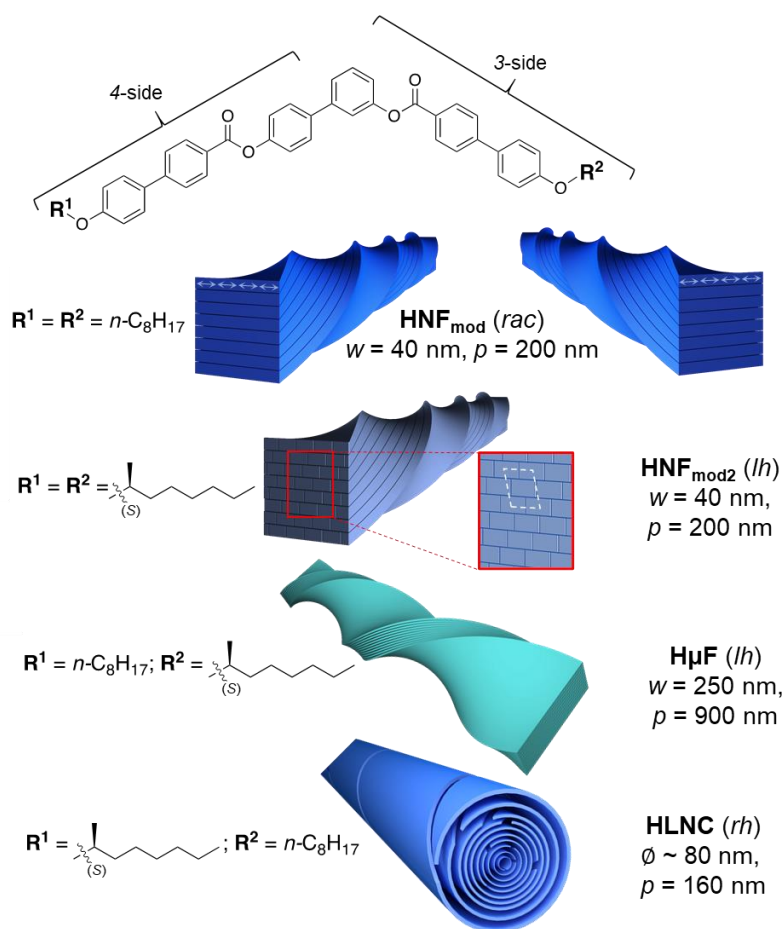


**Figure 10.** Bent-core compounds forming various B4 morphologies – helical nanofilament (HNF), helical microfilament (HF), heliconical-layered nanocylinders (HLNC) – as a function of the presence and position of stereogenic centers in the molecules. The width ( $w$ ), diameter ( $\phi$ ) and pitch distances ( $p$ ) for each structure are indicated. The double-ended arrows in the HNF<sub>mod</sub> fibers imply intralayer modulation. In the HNF<sub>mod2</sub> fibers the dotted white parallelogram suggests both the intra- and inter-layer variations. We thank warmly Torsten Hegmann (Kent State University) for providing images.

The formation of twisted crystals from polymers is very interesting in comparison to the helical nanofilaments from bent-core liquid crystals, because it is also a result of lamellar structure bending and often results in homochiral domains with fibers of similar dimensions and whose twisting depends greatly on conditions of fiber growth.<sup>[91]</sup> Homochiral spherulites formed by spontaneous resolution during melt crystallization of high-density polyethylene, for example, can be characterized with microfocus X-ray diffraction.<sup>[92]</sup> This technique is valuable in this case because the size of the X-ray beam is smaller than the lamellar twisting period. Using small- and wide-angle diffraction experiments, it was concluded that right-handed helicoids form when the crystalline stems of the lamellae are tilted to the right from the normal to the basal plane of the sheets. That observation fitted the hypothesis forwarded where unbalanced surface stresses were implied to explain the twisting.<sup>[62]</sup> The chirality of fibril twisting can also be probed optically, by measuring circular retardance in the case the pitch is much longer than the probing light wavelength.<sup>[93]</sup> In that case, for a variety of intrinsically chiral and achiral polymers, optical imaging of the core of the spherulites showed that achiral polymers have heterochiral spherulite cores, while intrinsically chiral polymers have homochiral twist in that location.

Interestingly, intrinsically chiral polymers can also exhibit oppositely twisted crystals. Studies on isothermal melt crystallized poly[(*R*)-3-hydroxyvalerate] used quantitative birefringence imaging to measure at each pixel the azimuth angle of the slow optical axis and the birefringence retardation.<sup>[94]</sup> That technique demonstrated that the polymer had two radial growth directions, the *a* and *b* axes of the polymer lamellae, that had only slightly dissimilar growth rates in the crystallization experiment, meaning that both situations could exist in the same spherulite. These different growth directions give twisted crystals whose morphologies have opposite handedness, and these domains coexist in spherulites. Modelling of the anisotropic surface stress-related bending confirmed that an identical bending direction could lead to opposite twisting handedness for different chiral polymers.<sup>[95]</sup>

Assembly of small molecules can also display this kind of reversal in aggregate morphological chirality as a function of the hierarchy of assembly.<sup>[96]</sup> This effect can be seen using the chiroptical signal that indicates unwinding of individual fibrils,<sup>[97]</sup> and union of helical fibrils to give superhelices.<sup>[98]</sup> Helical aggregates of amide-containing phospholipids were shown to form helical fibers which in turn aggregate to superhelices with opposite chirality, and relief of stress was inferred to explain this effect.<sup>[99]</sup> A similar situation appears to take place in a compound with a tris(2,2'-bipyridinium)benzenetricarboxamide core with three symmetrically attached tetrathiafulvalene (TTF) units, each one having two chiral chains pendent to them. The

material assembles into twisted birefringent fibers columns in solution.<sup>[100]</sup> Under slightly different cooling conditions, an inversion of optical activity was seen *en route* to twisted microscopic fibers (Figure 11).<sup>[101]</sup> This particular example shows how a non-amphiphilic molecule can lead to lamellar twisted structures, the electron micrograph in figure 10 shows lines along the stubby helices that clearly correspond to a layered structure. The supramolecular level nature of the aggregates in sheets is unclear at present.

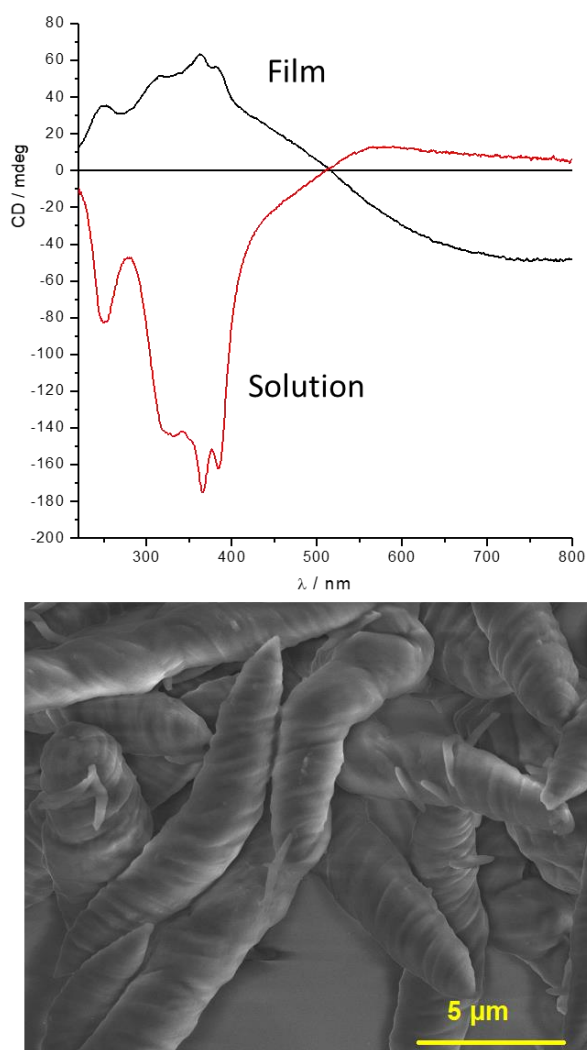


**Figure 11:** Circular dichroism spectra (top) of a solution of chiral  $C_3$  TTF-containing compound in dioxane (positive bands at 350 nm) and a film of the material on quartz (negative band at 350nm). The scanning electron micrograph (bottom) shows the twisted structures that are formed on cooling a solution of the compound, with lines corresponding to a layered structure evident.

Curved objects have been observed in the formation of aggregates at the water/air interface.<sup>[102]</sup> An early example is a simple amide derivative of single chain phospholipids form spiral-shape aggregates, whose morphology can be influenced with the pH of the

subphase, showing that modulation of the electrostatic and hydrogen bonding interactions in the layer can influence the degree of twisting.<sup>[103]</sup> Molecules that are similar in composition and constitution can show contrasting hierarchical superstructures at domain and morphology levels. For example, phospholipids with primary or quaternary ammonium group organize in very different ways as a result of the dipoles in the molecules.<sup>[104]</sup> Domains with triskelion-like curved arms are formed by the quaternary ammonium compound where the bending originates from the chirality of the head group. The primary ammonium compound shows domains containing curved defects separating areas of different orientation. The origin of the contrasting morphologies was explained by the different supramolecular interactions taking place between the surfactants in the monolayers on the basis of coarse-grained theoretical studies.<sup>[105]</sup> The more extended conformation of the quaternary ammonium surfactant leads to a bigger dipole than the primary derivative, especially in the plane of the film. It is interesting to note that single domains of phospholipid membranes can be probed with polarized two-photon fluorescence microscopy, where central vortices of one lipid in a two-component system can form.<sup>[106]</sup> In that case, the domains did not have a particular chiral morphology, but the appearance of the vortices was linked to the "hydrophobic mismatch" between the two components, that is related to the difference in length of the alkyl chains and the absence of a specific orientation at the boundary between the two materials.

Other interesting morphologies also appear in these low dimensional systems: The films formed by a chiral cyclobutane  $\beta$ -amino acid-based amphiphile gave dendritic structures that were chiral at the surface of water.<sup>[107]</sup> Brewster angle micrographs showed acicular objects with asymmetric dendritic branching, whereby the same handedness forking was observed throughout the film. This phenomenon was associated with the fact that the amphiphiles must form polar structures at the interface, with the hydrophilic groups in contact with the water, centrosymmetric structures are greatly unfavored.<sup>[108,109]</sup> The occurrence of chiral morphologies in two-component domains<sup>[110]</sup> suggests the breadth of asymmetric objects that can be created at interfaces.

### **Making twisted crystals**

The initial reports suggested that a relatively high proportion of a wide variety of substances might form twisted crystals under the right conditions.<sup>[19]</sup> That possibility has been confirmed by a broad study of twisted crystals grown from melts.<sup>[111]</sup> Remarkably, for 101 compounds selected at random, and of which many display polymorphism (to give a total of 155 known crystal structures), an approximate 31% could twist as they crystallized. The two main factors that govern the formation of the twisted crystals appear to be the formation of solids with high aspect ratios and the growth conditions, that in turn are dominated by temperature and additional compounds in the melt.

The effect of temperature is shown dramatically for hippuric acid,<sup>[24]</sup> that grows fibers along the [100] direction in the interval 80 to 180 °C and down the [001] axis between 60 and 115 °C. Both conditions give twisted crystals, albeit with different pitch. In the study on melts, large supercooling was preferable; if large crystals were grown by cooling to room temperature, rapid cooling in a refrigerator was tried. Similarly, increasing the concentration of additives could lead to higher aspect ratio crystals with a greater propensity to twist. Therefore, the turning growth depended on the crystal habit rather than the molecular structure, crystal structure and symmetry, that are apparently not directly related to the phenomena.

In this study on melts, chirality did not apparently play a determining role regarding the potential for forming twisted crystals, although the sense of twisting was affected by stereochemistry. D-Mannitol forms two polymorphs, which both have the same helical sense when twisted solids are formed using sorbitol as an additive, but which have opposite handedness when poly(vinylpyrrolidone) was used as the additive.<sup>[65]</sup> The achiral compound resorcinol – something of a classic in the twisted crystal literature – does form single handed morphologies when one enantiomer of tartaric acid is used as an additive, a helicity that is the opposite when the enantiomer of the crystal growth modifier is used.<sup>[112]</sup>

The majority of the compounds mentioned in these crystallizations from the melt studies had one important thing in common: a relatively low melting point. We have already seen that twisted crystals can also form from solution, benzamide being a highlighted case, and hippuric acid also forms twisted crystals from solvent growth. Another beautifully documented example is decacyclene.<sup>[113]</sup> The compound forms mesoscopic twisted ribbons when crystallized from 1:1 benzene-pinacolone. The helical twist of these objects was both left and right handed. They were assigned to the conformational enantiomers of the compound (a gently twisted three-bladed propeller) caused by the steric clash between hydrogen atoms on the naphthalene moieties (Figure 12). The twisting negated the solution of the X-ray structure of the solution grown sample, but sublimation afforded less distorted crystals that provided a solved form. The solid belongs to the chiral space group  $C222_1$ , so each crystal contains a single enantiomer. While definitive proof is awaited, on the basis that powder diffraction experiments proved that the crystal structure of the solution-grown twisted crystals and the sublimation formed ones was the same, the authors suggested that the oppositely twisted crystals correspond to mirror enantiomers of the propeller conformation.

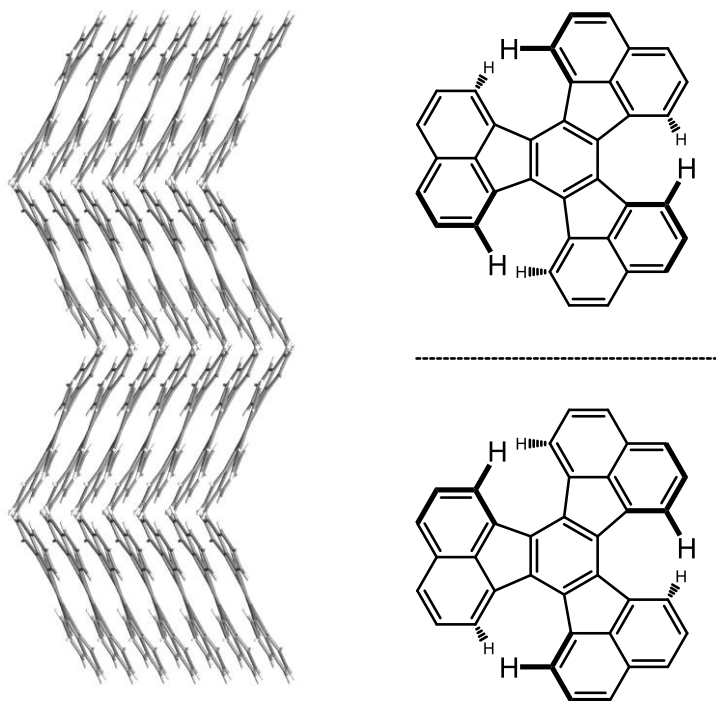


**Figure 12:** A view down the b axis of the decacyclene crystal structure and drawings of the conformational enantiomers in an exaggerated propeller shape.

Conformational enantiomers that do show opposite twists are those of benzil, where crystals pertaining to the enantiomorphous space groups,  $P3_121$  and  $P3_221$  are mirror images of one another.<sup>[114]</sup> To understand the origins of this twisting, molecular simulations were performed whereby benzil nanorods had right- and left-handed screw dislocations introduced. Simulations of the nanocrystals of benzil suggest twisting and therefore that they do not have a habitual crystallographic lattice.<sup>[115]</sup> The model then simulated the effects of introducing screw dislocations that went in the same sense as the helical twist, or against it. When screw dislocations were introduced in a positive or negative sense, for a given enantiomorph these would tend to twist further or to straighten the object, and this latter case was referred to as Eshelby untwisting. The effects are not equal in energetic terms, because the structures are both molecularly chiral and mechanically chiral. It was found that the nanorods that were untwisted had higher potential energy than those whose screw dislocation sense was in the same direction as the initial twist of the objects.

### Exotic chiral crystals

Enantiomorphous crystals can be remarkable, and it is worth highlighting examples of chiral morphologies that are particularly nice before concluding. One is a demonstration of the

Eshelby mechanism in action in the growth of germanium sulfide twisted van der Waals (vdW) nanowires with tailored twisting rates by controlling the size of the structure's diameter.<sup>[116]</sup> As the twisted structures were fixed to the silica-coated silicon substrates on which they were grown, with a chemical vapor transport method using gold as catalyst, further radial growth leads to an increase in elastic energy. That energy is relieved at a critical radial size by the slipping of nanoplates, a phenomenon permitted by the weak interlayer vdW bonding, giving a morphologically twisted nanowire with discrete jumps between plates. (Figure 13) The origin of the mesoscopic twist is Eshelby twisting of dislocated nanowires of about 200 nm diameter first generated by gold-catalyzed vapor-liquid-solid growth. The mesoscopic crystals have diameters from several hundred nanometers to greater than 10 microns, twist periods from 2 to 20 microns, and up to hundreds of microns in lengths, and the thickness of the periodically rotating nanoplates is several hundred nanometers. The method was shown to be general in the formation of stepped germanium selenide on the germanium sulfide nanowires.

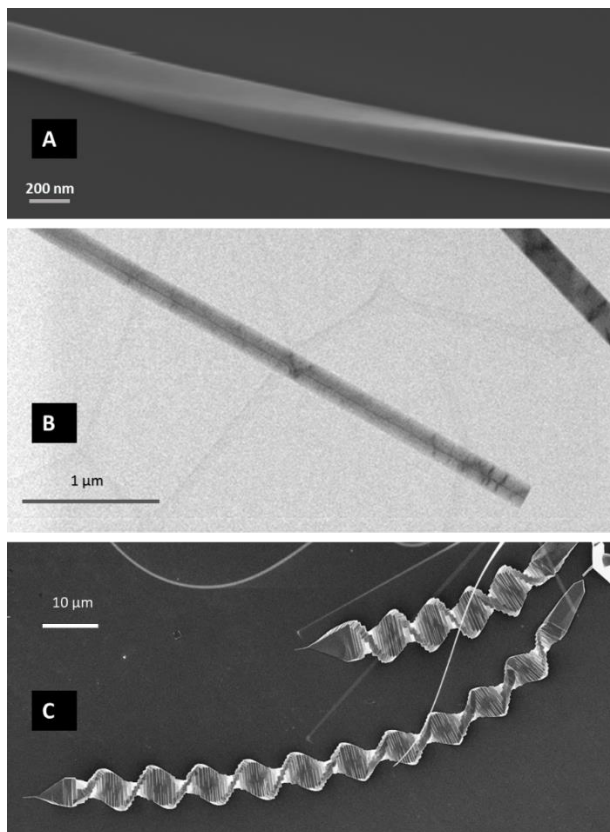


**Figure 13:** The growth of twisted germanium sulfide by firstly growing mesoscopically twisted dislocated nanowires with a gold-catalyzed vapor-liquid-solid method, shown by scanning (A) and transmission (B) electron microscopy, and the twisted objects formed by subsequent radial growth viewed with a scanning electron microscope (C). We warmly thank Jie Yao (University of California, Berkeley) for providing the images.

The remarkable crystallization of a tetrapodal ligand with tetrahedral geometry (based around an adamantane core) with copper(II) nitrate leads to metallo-organic single crystals with a chiral morphology comprising multiple domains (Figure 14).<sup>[117]</sup> The apparently separate domains all have an orientation consistent with the objects being a single crystal, that is traversed by spiral motifs in the morphological and crystallographic sense. The crystals were grown by an initial solvothermal reaction to generate nuclei, followed by two days to allow for crystal growth at room temperature. The origin of the chirality lies in the coordination geometry of the copper (II), where four pyridine moieties coordinate (along with two axially bound water molecules) and form a continuous coordination network that makes homochiral channels that are all the same sense for a given crystal that has a chiral morphology dependent on the chiral coordination sphere, while the bulk of the sample is a racemic conglomerate, as shown conclusively by X-ray diffraction (space group *P622*). The chirality arises from the propeller-type arrangement of the four pyridine moieties around the metal ion. It is a fascinating example of a non-polyhedral crystals with a chiral morphology and structure. The hexagonal pores that are formed are neighbored by six triangular channels (Figure 14), all of them being perpendicular to the wider surface of the crystals. It is, perhaps, reminiscent of naturally occurring biomaterials that form continuous structures. This example, and the previous one, highlight the opportunities arising from complicated crystallization processes where more than one step results in a non-trivial morphology.

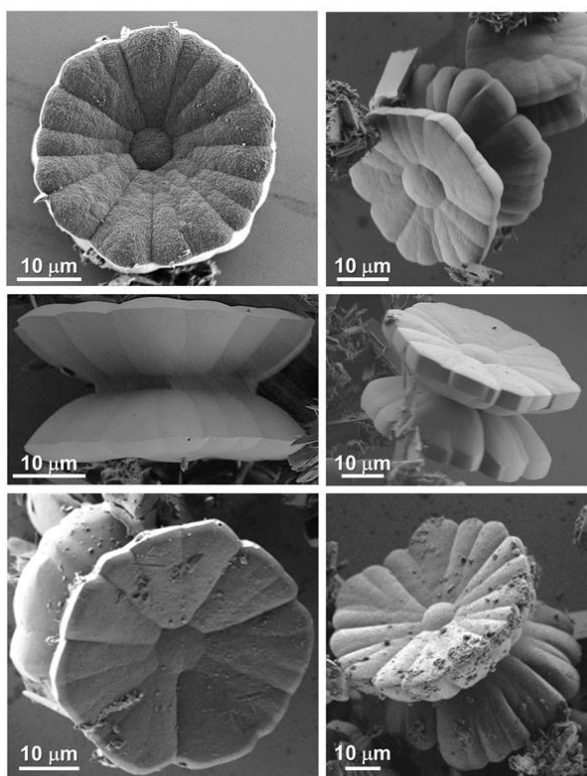
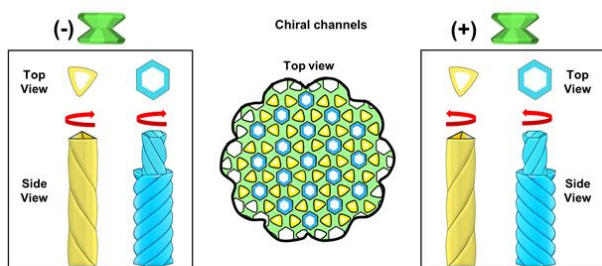


**Figure 14:** Top: The continuous hexagonal and triangular helicoidal channels that comprise each enantiopure crystal of a metallo-organic system based on copper(II) coordination by a tetrapodal ligand (the bulk sample is a racemic conglomerate). Below. Scanning electron micrographs of the yo-yo shaped crystals. We thank warmly Michal Lahav, Chiara Di Gregorio and Milko van der Boom (Weizmann Institute of Science) for supplying the images.

An interesting inorganic case of crystallographic and morphological chirality was also displayed when the cinnabar form of mercury sulfide was prepared in a two-step synthetic route.<sup>[118]</sup> Firstly, nanoparticle nuclei were prepared from the mercury sulfide precursors using either D- or L-penicillamine as capping ligands, and secondly the nuclei were used in an epitaxial growth procedure in the presence of additional precursors and ligand to form objects with a twisted bipyramid morphology. The material crystallizes in the enantiomorphic space groups  $P3_121$  or  $P3_221$  with right- or left-handed helices, respectively. The morphological handedness of the twist in the distorted bipyramids – that were approximately 20 nm long – correlates with the structural chirality of the seed. The

work built on related studies on tellurium, using a different procedure.<sup>[119]</sup> In both cases, very significant chiroptical activity, in the case of cinnabar modelling showed how distortion of the colloid affected these effects.

Chiral morphology can emerge by the addition of chiral growth modifiers. For example, during the formation of calcite crystals the selective binding of specific enantiomers of amino acids at surface steps in a surfactant-like manner leads chiral morphology induction.<sup>[120]</sup> The amino acid binding alters the free energy of the surface steps at the atomic scale, that has a macroscopic effect on the crystal growth. That phenomenon observed in the growth of calcite by the reaction of precursors to the mineral in solution can also be observed in the electrochemical deposition of the mineral in the presence of tartaric acid, albeit with different crystallographic steps being the subject of binding by the crystal growth modifier.<sup>[121]</sup> These examples form part of a much wider field where selective adsorption can lead to chiral growth of inorganic materials.<sup>[122]</sup>

The growth of mesoporous silica with both twisted external microscopic morphology and chiral channels in the crystals were prepared using chiral anionic surfactants as templates.<sup>[123]</sup> The aqueous-based procedure, involving room temperature templating followed by curing at 80 °C, produced twisted hexagonal rod-like objects 130-180 nm wide and 1–6 µm long. It is a beautiful example of how chirality can be transferred “through space and across length scales”.<sup>[124]</sup>

### **Twisting flat crystals**

While we have concentrated on the formation of twisted morphologies during crystal growth, it is possible to form twisted crystals from flat ones, and a brief mention of those is important. They are a route to generating strain through another route, far from equilibrium, requiring a chemical stimulus. This stress could be caused by an isomerization in the crystal or a covalent bond forming approach.<sup>[125]</sup> A very relevant case here is the topochemical reaction of azide and alkyne functional groups on a homochiral dipeptide to give a cycloaddition product in the solid that results in twisting of plank-like crystals.<sup>[126]</sup> After crystallization, over time and at room temperature and 0 °C, the LL enantiomer of the compound undergoes spontaneous twisting giving right-handed crystals (Figure 15). The tension resulting in the bending was proven to be a result of the covalent bond-forming reaction, whose rate can be increased by heating the crystals. The twisting direction is a result of the molecular chirality because the DD enantiomer’s crystals twist in the opposite sense. Furthermore, the rate of twisting was dependent on the thickness of the crystals, with thicker crystals taking much longer to distort. This beautiful experiment shows how reactions can induce strain and lead to twisted crystals, with the important condition that the functional groups are suitably located to be able to undergo the topochemical reaction.

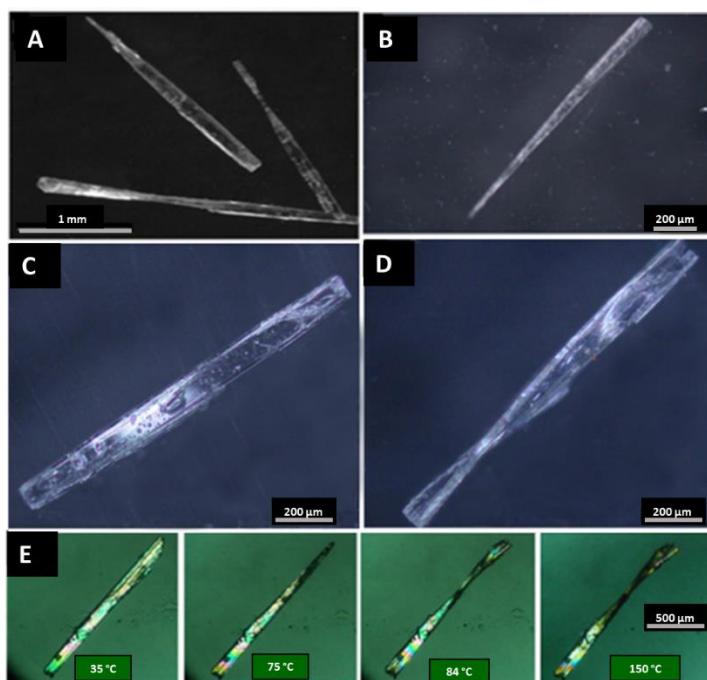


**Figure 15:** Photographic images of twisted crystals of a homochiral dipeptide (A) after 1 month at room temperature, (B) after 3 months at 0 °C, and (C) before and (D) after heating-induced reaction at 85 °C for 3 days. (E) Polarized micrographs of gradual twisting of crystals during heating on a hot-stage from 35 °C to 150 °C. We thank warmly Kana M. Sureshan (IISER Thiruvananthapuram) for providing the images.

### Concluding remarks and Outlook

It has been shown clearly that for certain sizes of crystals and under certain conditions twisting can be a remarkably common phenomenon. The belief that “the tendency for twist in the orientation of neighboring molecules is incompatible with ordering into a lattice”<sup>[86]</sup> does not stop that. While local strain in planar layers overcomes twisting in larger crystals (recall Figure 8) a huge number of materials can be solidified to give helical morphologies under certain conditions. Therefore, the idea of “geometrically frustrated assemblies”<sup>[127]</sup> might be even more general than presently considered.

The morphology of crystals is still hard to predict, even if it can be controlled. The occurrence of screw dislocations can give rise to transfer of chirality without the emergence of twisting or bending, and it has been suggested that they can also give rise to enantiomorphic shapes that are not curved, as shown for the case of tellurium nanocrystals.<sup>[128]</sup> Predicting morphology is hard, but theoretical approaches involving consideration of the solid-fluid interface have been known for some time,<sup>[129]</sup> although general use is infrequent and is necessarily on a case by case basis that perhaps limits the growth of the field.

The crystallization of chiral and achiral compounds into either conglomerates and racemic compounds has received great attention, even if the phenomenon is not entirely understood in many cases it can be controlled and used, for example for the resolution of enantiomers. The emergence of morphological chirality during the precipitation of materials is often not considered in this context and perhaps deserves attention. This challenge is perhaps even more pertinent for macromolecules, where explaining exactly how polymers crystallize is an ongoing challenge,<sup>[130]</sup> and as we pointed out earlier, there may be synergies between the twisting of small molecule supramolecular assemblies and polymer ribbons.

Apart from the extraordinary science waiting to be discovered for twisted crystals, for certain present applications of organic solids flowability, filterability and density can be important, and the formation of spherulites using an additive, as in the case of L-valine, can be advantageous.<sup>[131]</sup> The twisted morphology may also bring opportunities in molecular electronics.<sup>[132,133]</sup> The morphological chirality of crystals has also been shown to be transferred into reactions carried out in their presence, in the case of the Soai reaction.<sup>[134,135]</sup> Away from organic compounds, the area of chiral nanoceramics is a burgeoning area that benefits from controlled growth of twisted crystals.<sup>[136]</sup> There are even suggestions that the passage of chirality between macroscopic objects, rather than single molecules, could have had an influence on the emergence of homochirality in biological systems.<sup>[137]</sup> Whatever the case, there are many opportunities in the exploration of twisted crystals.

## Acknowledgements

The authors warmly thank Mònica Amabilino i Pérez for the photographs in Figure 2, Michal Lahav, Maria Chiara Di Gregorio and Milko van der Boom (Weizmann Institute of Science), Kana M. Sureshan (IISER Thiruvananthapuram), Torsten Hegmann (Kent State University), and Jie Yao (University of California, Berkeley) for providing images of their beautiful research results. CEK thanks the LDMI DTP and the University of Nottingham for funding.

## References

- [1] L. Pasteur, *Ann. Chim. Phys.*, **1848**, 24, 442-459.
- [2] Y. Tobe, *Mendeleev Commun.*, **2003**, 93-94.
- [3] J. Gal, *Chirality*, **2008**, 20, 5-19.

- [4] J.M. Bijvoet, A.F. Peerdeman, A.J. van Bommel. *Nature*, **1951**, 168, 271–272.
- [5] H.D. Flack, *Helv. Chim. Acta*, **2003**, 86, 905-921.
- [6] V. Bisker-Leib and M.F. Doherty, *Cryst. Growth Des.*, **2003**, 3, 221-237
- [7] K. Tanaka, T. Iwamoto, S.-I. Wada, J. Frelek, M.R. Caira, *Chirality*, **2006**, 18, 483–488.
- [8] O. Hager, A.L. Llamas-Saiz, C. Foces-Foces, R.M. Claramunt, C. López, J. Elguero, *Helv. Chim. Acta*, **1999**, 82, 2213-2230.
- [9] D.B. Amabilino, R.M. Kellogg, *Isr. J. Chem.*, **2011**, 51, 1034-1040.
- [10] C. Viedma, *Phys. Rev. Lett.*, **2005**, 94, 065504.
- [11] L.-C. Sögütöglu, R.R.E. Steendam, H. Meekes, E. Vlieg, F.P.J.T. Rutjes, *Chem. Soc. Rev.*, **2015**, 44, 6723-6732.
- [12] L. Addadi, S. Weiner, *Nature*, **2001**, 411, 753-754.
- [13] I. Weissbuch, L. Leiserowitz, M. Lahav, *Chirality*, **2008**, 20, 736/748.
- [14] L. Addadi, Z. Berkovitch-Yellin, I. Weissbuch, M. Lahav, L. Leiserowitz, *J. Am. Chem. Soc.*, **1982**, 104, 2075-2077.
- [15] Z. Berkovitch-Yellin, L. Addadi, M. Idelson, L. Leiserowitz, M. Lahav, *Nature*, **1982**, 296, 27-34.
- [16] L. Addadi, Z. Berkovitch-Yellin, N. Domb, E. Gati, M. Lahav, L. Leiserowitz, *Nature*, **1982**, 296, 21-26.
- [17] O. Lehmann, *Molekularphysik mit besonderer berücksichtigung mikroskopischer untersuchungen und anleitung zu solchen sowie einem anhang über mikroskopische analyse*, Leipzig W. Engelmann 1888.
- [18] A. G. Shtukenberg, Y. O. Punin, A. Gujural and B. Kahr, *Angew. Chem. Int. Ed.*, **2014**, 53, 672-699.
- [19] F. Bernauer, "*Gedrilte*" Kristalle: Verbreitung, Entstehungsweise und Beziehungen zu optischer Aktivitat und Molekulasymmetrie, Gebrüder Borntraeger, Berlin, 1929.
- [20] L. J. Spencer, *Mineral. Mag.*, **1921**, 19, 263–274.
- [21] A. W. Weitkamp, *J. Am. Chem. Soc.*, **1945**, 67, 447–454.
- [22] B. W. Hotten, D. H. Birdsall, *J. Colloid Sci.*, **1952**, 7, 284–294.
- [23] T. Tachibana, H. Kambara, *J. Am. Chem. Soc.*, **1965**, 87, 3015–3016.

- [24] A. Shtukenberg, E. Gunn, M. Gazzano, J. Freudenthal, E. Camp, R. Sours, E. Rosseeva, B. Kahr, *ChemPhysChem*, **2011**, *12*, 1558-1571.
- [25] O. Giraldo, S.L. Brock, M. Marquez, S.L. Suib, H. Hillhouse, M. Tsapatsis, *Nature*, **2000**, *405*, 38-38.
- [26] M. Yang, N. Kotov, *J. Mater. Chem.*, **2011**, *21*, 6775-6792.
- [27] C. Li, D. Yan, S. Cheng, F. Bai, T. He, L. Chien, F. W. Harris, B. Lotz, *Macromolecules*, **1999**, *32*, 524-527.
- [28] C. Kübel, D. P. Lawrence, D. C. Martin, *Macromolecules*, **2001**, *34*, 9053-9058.
- [29] D.M. Ho, R.A. Pascal, Jr., *Chem. Mater.*, **1993**, *5*, 1358-1361.
- [30] A. G. Shtukenberg, A. Gujral, E. Rosseeva, X. Cui, B. Kahr, *Cryst. Eng. Comm.*, **2015**, *17*, 8817-8824.
- [31] F. C. Frank, *Discuss. Faraday Soc.*, **1949**, *5*, 48-54.
- [32] W. K. Burton, N. Cabrera, F. C. Frank, *Nature*, **1949**, *163*, 398-899.
- [33] J. D. Eshelby, *J. Appl. Phys.*, **1953**, *24*, 176-179.
- [34] W. W. Webb, W. D. Forgent, *J. Appl. Phys.*, **1957**, *29*, 251-261.
- [35] R. D. Dragsdorf, W. W. Webb, *J. Appl. Phys.*, **1958**, *29*, 817-819.
- [36] G. W. Sears, *J. Chem. Phys.*, **1959**, *31*, 53-54.
- [37] B. Jeszyszky, E. Hartmann, *Nature*, **1961**, *189*, 213.
- [38] S. A. Morin, S. Jin, *Nano Lett.*, **2010**, *10*, 3459-3463.
- [39] J. Zhu, H. Peng, A. F. Marshall, D. M. Barnett, W. D. Nix, Y. Cui, *Nat. Nanotechnol.*, **2008**, *3*, 477-481.
- [40] M. J. Bierman, Y. K. A. Lau, A. V. Kvit, A. L. Schmitt, S. Jin, *Science*, **2008**, *320*, 1060-1063.
- [41] F. Meng, S.A. Morin, A. Forticaux, S. Jin, *Acc. Chem. Res.*, **2013**, *46*, 1616-1626.
- [42] J. M. Schultz, D. R. Kinloch, *Polymer*, 1969, *10*, 271-278; H. D. Keith, W. Y. Chen, *Polymer*, **2002**, *43*, 6323-6272.
- [43] N. Hirai, *J. Polym. Sci.*, **1962**, *59*, 321-328.
- [44] D. C. Basset, *Phil. Trans. R. Soc. Lond. A*, **1994**, *348*, 29-34.

- [45] A. Toda, M. Okamura, K. Taguchi, M. Hikosaka, H. Kajioka, *Macromolecules*, **2008**, *41*, 2482-2493.
- [46] J. Xu, B-H. Guo, Z-M. Zhang, J-J. Zhou, Y. Jiang, S. Yan, L. Li, Q. Wu, G-Q. Chen, J. M. Schultz, *Macromolecules*, **2004**, *37*, 4118-4123.
- [47] B. Shen, B. Liang, X. Wang, P-C. Chen, C. Zhou, *ACS Nano*, **2011**, *5*, 2155-2161.
- [48] R. Yang, Z. L. Wang, *J. Am. Chem. Soc.*, **2006**, *128*, 1466-1467;
- [49] G. Z. Shen, Y. Bando, C. Y. Zhi, X. L. Yuan, T. Sekiguchi, D. Golberg, *Appl. Phys. Lett.*, **2006**, *88*, 243106.
- [50] G. Shen, D. Chen, *J. Am. Chem. Soc.*, **2006**, *36*, 112762-11763.
- [51] R. Yang, Z. L. Wang, *J. Am. Chem. Soc.*, **2006**, *128*, 1466-1467.
- [52] H. Wang, J-C. Wu, Y. Shen, G. Li, Z. Zhang, G. Xing, D. Guo, D. Wang, Z. Dong, T. Wu, *J. Am. Chem. Soc.*, **2010**, *132*, 15875-15877.
- [53] X. Y. Kong, Z. L. Wang, *Nano Lett.*, **2003**, *3*, 1625-1631.
- [54] R. Yang, Y. Ding, Z. L. Wang, *Nano Lett.*, **2004**, *4*, 1309-1312.
- [55] P. X. Gao, Y. Ding, W. Mai, W. L. Highes, C. Lao, Z. L. Wang, *Science*, **2005**, *309*, 1700-1704.
- [56] P. Z. Gao, W. Mai, Z. L. Wang, *Nano Lett.*, **2006**, *11*, 2536-2543.
- [57] X. Y. Kong, Z. L. Wang, *Nano Lett.*, **2003**, *3*, 1625-1631.
- [58] B. Lotz, S. Z. D. Cheng, *Polymer*, **2005**, *46*, 577-610.
- [59] D. C. Basset, *Polymer*, **2006**, *47*, 3263-3266.
- [60] ref Y. Fujiwara, *J. Appl. Polym. Sci.*, **1960**, *4*, 10-15.
- [61] A. Keller, *J. Polym. Sci.*, **1959**, *39*, 151-173.
- [62] H. Keith and F. Padden, *Macromolecules*, **1996**, *29*, 7776-7786.
- [63] A. Lovinger, *Macromolecules*, **2020**, *53*, 741-745
- [64] S. Nagarajan, E.M. Woo, *Macromol. Rapid Commun.*, **2021**, *42*, 2000708.
- [65] A. G. Shtukenberg, X. Cui, J. Freudenthal, E. Gunn, E. Camp, B. Kahr, *J. Am. Chem. Soc.*, **2012**, *134*, 6354-6364.
- [66] Y. O. Punin, *J. Struct. Chem.*, **1994**, *35*, 616-624.

- [67] Y. O. Punin, O. I. Artamonova, *Cryst. Rep.*, **2001**, *43*, 138-143.
- [68] A. G. Shtunkenberg, R. Drori, E. V. Sturn, N. Vidavsky, A. Haddad, J. Zheng, L. A. Estroff, H. Weissman, S. G. Wolf, E. Shimoni, C. Li, N. Fella, E. Efrati, B. Kahr, *Angew. Chem. Int. Ed.*, **2020**, *59*, 14593-14601.
- [69] A. G. Shtunkenberg, J. Freudenthal, B. Kahr, *J. Am. Chem. Soc.*, **2010**, *132*, 9341-9349.
- [70] G. G. Laemlein, *Izv. Akad. Nauk SSSR, Ser. Geol.*, **1937**, 937-964.
- [71] Y. O. Punin, A. G. Shtunkenberg, *Autodeformation Defects in Crystals*, St. Petersburg Univ. Press, St. Petersburg, Russia, 2008.
- [72] J. Suda, M. Matsushita, *J. Phys. Soc. Jpn.*, **1995**, *64*, 348-351.
- [73] H. Imai, Y. Oaki, *Angew. Chem., Int. Ed.*, **2004**, *43*, 1363-1368.
- [74] K. Kawabata, T. Kumagai, M. Mizutani, T. Sambongi, *J. Phys. I*, **1996**, *6*, 1575-1580.
- [75] P. D. Calvert, D. R. Uhlmann, *J. Polym. Sci., Part B: Polym. Phys.*, **1973**, *11*, 457-465.
- [76] A. Brizard, R. Oda, I. Huc, *Top. Curr. Chem.*, **2005**, *256*, 167-218.
- [77] M. Liu, L. Zhang, T. Wang, *Chem. Rev.*, **2015**, *115*, 7304-7397.
- [78] E. Yashima, N. Ousaka, D. Taura, K. Shimomura, T. Ikai, K. Maeda, *Chem. Rev.*, **2016**, *116*, 13752-13990.
- [79] J.H. Fuhrhop, W. Helfrich, *Chem. Rev.*, **1993**, *93*, 1565-1582.
- [80] A. Sorrenti, J. Leira-Iglesias, A.J. Markvoort, T.F.A. de Greef, T.M. Hermans, *Chem. Soc. Rev.*, **2017**, *46*, 5476-5490.
- [81] J. Matern, Y. Dorca, L. Sánchez, G. Fernández, *Angew. Chem. Int. Ed.*, **2019**, *58*, 16730-16740.
- [82] M. Samperi, L. Perez-Garcia, D.B. Amabilino, *Chem. Sci.*, **2019**, *10*, 10256-10266.
- [83] E.T. Pashuck, S.I. Stupp, *J. Am. Chem. Soc.*, **2010**, *132*, 8819-8821.
- [84] T.J. Moyer, H. Cui, S.I. Stupp, *J. Phys. Chem. B*, **2013**, *117*, 4604-4610.
- [85] G. Zaldivar, M. Conda-Sheridan, M. Tagliazucchi, *J. Phys. Chem. B*, **2020**, *124*, 3221-3227.

- [86] L.E. Hough, H.T. Jung, D. Krüerke, M.S. Heberling, M. Nakata, C.D. Jones, D. Chen, D.R. Link, J. Zasadzinski, G. Heppke, J.P. Rabe, W. Stocker, E. Körblova, D.M. Walba, M.A. Glaser, N. A. Clark, *Science*, **2009**, *325*, 456-460.
- [87] L. Pérez-García, D.B. Amabilino, *Chem. Soc. Rev.*, **2002**, *31*, 342-356
- [88] L. Pérez-García, D.B. Amabilino, *Chem. Soc. Rev.*, **2007**, *36*, 941-967.
- [89] J. Liu, S. Shadpour, M.E. Prévôt, M. Chirgwin, A. Nemati, E. Hegmann, R.P. Lemieux, T. Hegmann, *ACS Nano*, **2021**, *15*, 7249–7270.
- [90] S. Shadpour, A. Nemati, M. Salamończyk, M.E. Prévôt, J. Liu, N.J. Boyd, M.R. Wilson, C. Zhu, E. Hegmann, A.I. Jákli, T. Hegmann, *Small*, **2020**, *16*, 1905591.
- [91] J. Xu, S. Zhang, B. Guo, *Chinese Chem. Lett.*, **2017**, *28*, 2092–2098.
- [92] M. Rosenthal, G. Bar, M. Burghammer, D.A. Ivanov, *Angew. Chem. Int. Ed.*, **2011**, *50*, 8881–8885.
- [93] H.-M. Ye, H.-M. Ye, J.H. Freudenthal, M. Tan, J. Yang, B. Kahr, *Macromolecules*, **2019**, *52*, 8514–8520.
- [94] H.-M. Ye, J. Xu, B.-H. Guo, T. Iwata, *Macromolecules*, **2009**, *42*, 694–701.
- [95] H.-M. Ye, J.-S. Wan, S. Tang, J. Xu, X.-Q. Feng, B.-H. Guo, X.-M. Xie, J.-J. Zhou, L. Li, Q. Wu, G.-Q. Chen, *Macromolecules*, **2010**, *43*, 5762–5770.
- [96] V. A. Tverdislov, E. V. Malysheko, *Physics Uspekhi*, **2019**, *62*, 354-363.
- [97] A. Sharma, J.P. Wojciechowski, Y. Liu, T. Pelras, C. M. Wallace, M. Müllner, A. Widmer-Cooper, P. Thordarson, G. Lakhwani, *Cell Reports Phys. Sci.*, **2020**, *1*, 100148.
- [98] M. Hifsudheen, R.K. Mishra, B. Vedhanarayanan, V.K. Praveen, A. Ajayaghosh, *Angew. Chem. Int. Ed. Engl.*, **2017**, *56*, 12634–12638.
- [99] N.A.J.M. Sommerdijk, P.J.J.A. Buynsters, H. Akdemir, D.G. Geurts, A.M.A. Pistorius, M.C. Feiters, R.J.M. Nolte, B. Zwanenburg, *Chem. Eur. J.*, **1998**, *4*, 127-136.
- [100] I. Danila, F. Riobé, F. Piron, J. Puigmartí-Luis, J.D. Wallis, M. Linares, H. Ågren, D. Beljonne, D.B. Amabilino, N. Avarvari, *J. Am. Chem. Soc.*, **2011**, *133*, 8344–8353.
- [101] I. Danila, F. Pop, C. Escudero, L.N. Feldborg, J. Puigmartí-Luis, F. Riobé, N. Avarvari, D.B. Amabilino, *Chem. Commun.*, **2012**, *48*, 4552-4554.
- [102] N. Nandi and D. Vollhardt, *Chem. Rev.*, **2003**, *103*, 4033-4075.

- [103]N.A.J.M. Sommerdijk, P.J.A.A. Buynsters, A.M.A. Pistorius, M. Wang, M.C. Feiters, R.J.M. Nolte, B. Zwanenburg, *J. Chem. Soc., Chem. Commun.*, **1994**, 1941-1942.
- [104]K. Thirumoorthy, N. Nandi and D. Vollhardt, *Langmuir*, **2007**, *23*, 6991-6996.
- [105]N. Nandi and D. Vollhardt, *J. Phys. Chem. B*, **2002**, *106*, 10144-10149.
- [106]J. Dreier, J. Brewer, A.C. Simonsen, *Langmuir*, **2014**, *30*, 10678–10685.
- [107]A. Sorrenti, O. Illa, R.M. Ortuño, R. Pons, *Langmuir*, **2016**, *32*, 6977–6984.
- [108]I. Weissbuch, I. Kuzmenko, M. Berfeld, L. Leiserowitz, M. Lahav, *J. Phys. Org. Chem.*, **2000**, *13*, 426-434.
- [109]F. Hoffmann, K.J. Stine, H. Hühnerfuss, *J. Phys. Chem. B*, **2005**, *109*, 240–252.
- [110]C. Rubia-Payá, J.J. Giner-Casares, M.T. Martín-Romero, D. Möbius, L. Camacho, *J. Phys. Chem. C*, **2014**, *118*, 10844–10854.
- [111]A.G. Shtukenberg, X. Zhu, Y. Yang, B. Kahr, *Cryst. Growth Des.* **2020**, *20*, 6186–6197.
- [112]B. Kahr, A. Shtukenberg, E. Gunn, D.J. Carter, A.L. Rohl, *Cryst. Growth Des.*, **2011**, *11*, 2070–2073.
- [113]D.M. Ho, R.A. Pascal Jr, *Chem. Mater.*, **1993**, *5*, 1358-1361.
- [114]X. Zhong, H. Zhou, C. Li, A.G. Shtukenberg, M.D. Ward, B. Kahr, *Chem. Commun.* **2021**, *57*, 5538–5541.
- [115]C. Li, A.G. Shtukenberg, L. Vogt-Maranto, E. Efrati, P. Raiteri, J.D. Gale, A.L. Rohl, B. Kahr, *J. Phys. Chem. C*, **2020**, *124*, 15616–15624.
- [116]Y. Lui, J. Wang, S. Kim, H. Sun, F. Yang, Z. Fang, N. Tamura, R. Zhang, Z. Song, J. Wen, B. Z. Xu, M. Wang, S. Lin, Q. Yu, K. B. Tom, Y. Deng, J. Tuner, E. Chan, D. Jin, R. O. Ritchie, A. M. Minor, D. C. Chrzan, M. C. Scott, J. Yao, *Nature*, **2019**, *570*, 358-362
- [117]M.C. di Gregorio, L.J.W. Shimon, V. Brumfeld, L. Houben, M. Lahav, M.E. van der Boom, *Nat. Commun.*, **2020**, *11*, Art. No. 380.
- [118]P.-P. Wang, S.-J. Yu, A.O. Govorov, M. Ouyang, *Nat. Commun.*, **2017**, *8*, Art. No. 14312
- [119]A. Ben-Moshe, S.G. Wolf, M.B. Sadan, L. Houben, Z. Fan, A.O. Govorov, G. Markovich, *Nat. Commun.*, **2014**, *5*, Art. No. 4302.

- [120]C.A. Orme, A. Noy, A. Wierzbicki, M.T. McBride, M. Grantham, H.H. Teng, P.M. Dove J.J. DeYoreo, *Nature*, **2001**, *411*, 775-779.
- [121]E.A. Kulp, J.A. Switzer, *J. Am. Chem. Soc.*, **2007**, *129*, 15120-15121.
- [122]S.W. Im, H.-Y. Ahn, R.M. Kim, N.H. Cho, H. Kim, Y.-C. Lim, H.-E. Lee, K.T. Nam, *Adv. Mater.*, **2020**, *32*, Art. No. 1905758.
- [123]S. Che, Z. Liu, T. Ohsuna, K. Sakamoto, O. Terasaki, T. Tatsumi, *Nature*, **2004**, *429*, 281-284.
- [124]S.M. Morrow, A.J. Bissette, S.P. Fletcher, *Nat. Nanotechnol.*, **2017**, *12*, 410-419.
- [125]Q. Yu, B. Aguila, J. Gao, P. Xu, Q. Chen, J. Yan, D. Xing, Y. Chen, P. Cheng, Z. Zhang, S. Ma, *Chem. Eur. J.*, **2019**, *25*, 5611-5622.
- [126]R. Raia, B.P. Krishnana, K.M. Sureshan, *PNAS*, **2018**, *115*, 2896-2901.
- [127]G.M. Grason, *J. Chem. Phys.*, **2016**, *145*, 110901.
- [128]A. Ben-Moshe, A. da Silva, A. Müller, A. Abu-Odeh, P. Harrison, J. Waelder, F. Niroui, C. Ophus, A.M. Minor, M. Asta, W. Theis, P. Ercius, A.P. Alivisatos, *Science*, **2021**, *372*, 729-733.
- [129]X. Y. Liu, E.S. Boek, W. J. Briels, P. Bennema, *Nature*, **1995**, *374*, 342-345.
- [130]X. Tang, W. Chen, L. Li, *Macromolecules*, **2019**, *52*, 3575- 3591.
- [131]W. Li, J. Yang, S. Du, E. Macaringue, Y. Wang, S. Wu, J. Gong, *Ind. Eng. Chem. Res.*, **2021**, *60*, 6048-6058.
- [132]A. Ajayaghosh, R. Varghese, S.J. George, C. Vijayakumar, *Angew. Chem. Int. Ed.*, **2006**, *45*, 1141-1144.
- [133]Y. Yang, Y. Zhang, Z. Wei, *Adv. Mater.*, **2013**, *25*, 6039-6049.
- [134].A. Matsumoto, H. Ozaki, S. Tsuchiya, T. Asahi, M. Lahav, T. Kawasaki, K. Soai, *Org. Biomol. Chem.*, **2019**, *17*, 4200-4203.
- [135]D.J. Carter, A.L. Rohl, A. Shtukenberg, S. Bian, C. Hu, L. Baylon, B. Kahr, H. Mineki, K. Abe, T. Kawasaki, K. Soai, *Cryst. Growth Des.*, **2012**, *12*, 2138-2145.
- [136]J. Fan, N.A. Kotov, *Adv. Mater.*, **2020**, *32*, Art. No. 1906738.
- [137]V.A. Tverdislov, E.V. Malyshko, *Symmetry*, **2020**, *12*, Art. No. 587.



Lizzie Killalea received her MSci degree from the University of Nottingham, UK, and continued there for her postgraduate studies with David Amabilino. Her PhD research covers the self-assembly of asymmetric chromophores, including the formation of twisted crystals.



David Amabilino received both BSc and PhD from Royal Holloway College (University of London). He is presently EPSRC/GSK Professor of Sustainable Chemistry at the University of Nottingham, where his group work on a variety of materials, including chiral ones.